TIME-FREQUENCY ANALYSIS BASED ON THE PHASE-RECTIFIED SIGNAL AVERAGING METHOD

Meryem Jabloun, Jérôme Van Zaen and Jean-Marc Vesin

EPFL, Signal Processing Institute (LTS1), Lausanne, 1015 CH, Swizerland.
E-mail addresses: firstname.lastname@epfl.ch, URLs: www.epfl.ch.

ABSTRACT

Phase rectified signal averaging (PRSA) is a technique recently introduced that outperforms the classical Fourier analysis when applied to nonstationary signals corrupted by impulsive noise. Indeed, the PRSA helps enhance quasi-periodic components in nonstationary signals while artifacts, intermittent components and high level noise are canceled. Thus the frequency estimation is improved.

In this paper, we introduce a new time-frequency representation (PRSA-TFR) which is obtained by applying the PRSA to sliding windows along the signal. This PRSA-TFR keeps the advantages of the PRSA and displays the time evolution of significant frequency components.

The comparison with classical time-frequency representations, such as the spectrogram and the Smoothed Pseudo-Wigner-Ville (SPWV) distribution, illustrates the potential of the PRSA-TFR to better reduce the noise level and to make the interpretation of the time-frequency features of the signal easier. The interest of the PRSA-TFR for real signals is illustrated on an electroencephalogram signal.

1. INTRODUCTION

In many applications such as mechanics, radar, sonar, wireless communications, speech processing and biomedical engineering, one is interested in the time evolution of frequency contents of nonstationary signals. The standard Fourier analysis is not useful for analyzing these nonstationary signals. Indeed, information which is localized in time such as impulsive noise and high frequency bursts cannot be easily detected and removed from the Fourier transform.

The time-frequency localization can be achieved by using the Cohen distributions which are bilinear and covariant time-frequency representations (TFR) [1, 2]. We mention the example of the spectrogram and the Smoothed Pseudo-Wigner-Ville distribution [1]. Nevertheless, these classical TFRs not only present a lack of resolution due to the Heisenberg-Gabor principle but they are inefficient in the presence of impulsive noise. Several techniques have been proposed to improve the TFR resolution such as the reassignment method [3, 4, 5] and the matching of TFRs with unitary warping operators [6].

In this paper, our main contribution is to better characterize time-frequency domain events for real signals which are corrupted by artifacts and impulsive noise. We define a new TFR based on the PRSA, a recently introduced technique [7] based on a simple principle. When applied to a nonstationary signal, the PRSA helps enhance existing quasi-periodic components that are hidden in a classical Fourier transform of the signal. The intermittent components, artifacts and noise are reduced, which improves frequency estimation.

The time-frequency analysis proposed is performed by first windowing the signal, so as to isolate only well-localized slices, and then by applying to them the PRSA [7]. This gives rise to the windowed PRSA transform. The magnitude of the PRSA transform is called the PRSA-TFR. This new TFR uses the ability of PRSA to capture the local periodicities and to improve the estimation of the frequency components underlying their time evolution.

The paper is organized as follows. The PRSA principle is described and the PRSA-TFR is introduced in Section 2. Results and discussions are presented in Section 3 for simulated signals and an electroencephalogram (EEG) signal. The final section concludes with a summary and some perspectives on our study.

2. PRSA AND TIME-FREQUENCY REPRESENTATION

2.1 A short introduction to PRSA

The basic idea of PRSA is very simple and consists in averaging selected segments of the studied signal y. These segments are symmetric regarding to so-called anchor points, samples at which the instantaneous phase of y is close to zero. The averaging process leads to a new signal, 'PRSA signal', the Fourier transform of which is called 'PRSA transform'.

Thanks to the averaging process, the PRSA method acts as a rejection filter of possibly correlated and nonperiodic components in the signal (such as noise and artifacts). On the other hand the quasi-periodic components of the initial signal y are conserved and enhanced.
In the following, the simplest version of PRSA is described [7]. The steps of the PRSA are illustrated in Fig.1.

The anchor points correspond to the increases in the real signal y (Fig.1(b)), i.e. instants n such that

$$y_n > y_{n-1}. \tag{1}$$

Assuming a total of M anchor points indexed by n_m, $m = 1,\ldots,M$, segments of length $2L+1$ are centered on these anchor points (Fig.1(c-e)),

$$\left[y_{n_m-L}, y_{n_m-L+1}, \ldots, y_{n_m}, \ldots, y_{n_m+L-1}, y_{n_m+L}\right]. \tag{2}$$

All these segments are averaged, which leads to the PRSA signal $\tilde{y}_\ell$

$$\tilde{y}_\ell = \frac{1}{M}\sum_{m=1}^{M} y_{n_m+\ell}, \qquad \text{for} \qquad \ell = -L, -L+1, \ldots, L. \tag{3}$$

The PRSA transform is the discrete Fourier transform (DFT) of the PRSA signal (3) and it is denoted by $\tilde{Y}_q$,

$$\tilde{Y}_q = \sum_{\ell=0}^{2L} \tilde{y}_{\ell-L}\ e^{-j2\pi\frac{q}{Q}\ell}, \qquad \text{for} \qquad q = 0, 1, \ldots, Q-1, \tag{4}$$

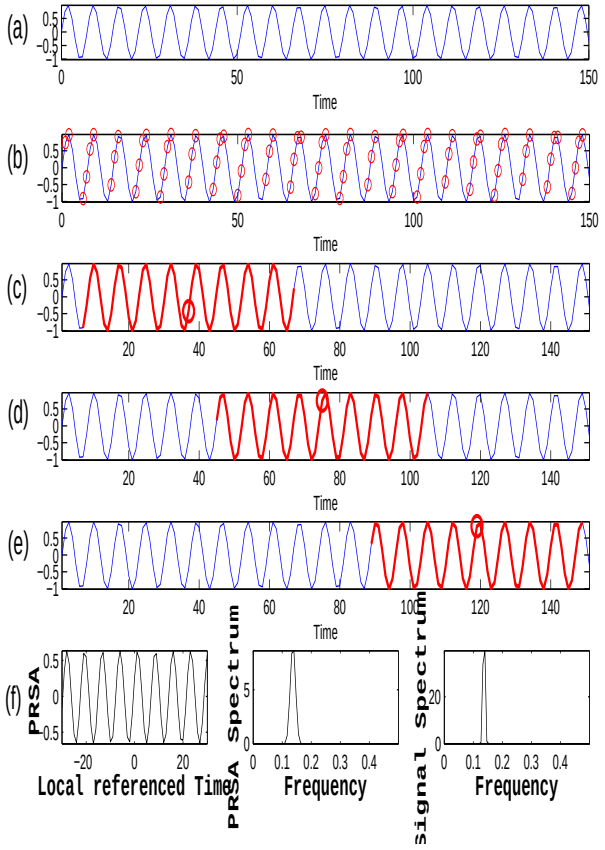

Figure 1: Principle of PRSA: (a) signal $y_n = \sin(2\pi 0.14n)$, (b) Anchor points, (c)-(e) Segments of length $2L+1 = 61$ centered on anchor points, (f) (left side) PRSA signal $\tilde{y}_\ell$ (3), (center) squared magnitude of the PRSA Transform $|\tilde{Y}_q|^2$ (4) and (right side) signal spectrum.

where $\frac{q}{Q}$ is the discrete frequency and Q is the DFT size.

To illustrate the potential of the PRSA, let us consider the following signal y defined by:

$$\begin{aligned} y_n &= \sin(2\pi 0.23n) + \sin(2\pi 0.29n) + \\ &\quad 15\sin\left(2\pi(0.02n^2 + 0.01n)\right)\mathbb{I}_{[50,100]}(n) + \\ &\quad 2\sin(2\pi 0.001n^2))\mathbb{I}_{[800,840]}(n) + Imp(n), \end{aligned} \tag{5}$$

where $\mathbb{I}_{[a,b]}$ is the indicator of the time interval $[a,b]$. y is composed of the sum of two sinusoids at frequencies 0.23 Hz and 0.29 Hz, the sampling Frequency is $F_s = 1$Hz. The signal is contaminated by an impulsive noise Imp and two intermittent frequency-modulated components.
As can be observed from Fig.2(c), the frequency peak at 0.29 Hz is clearly enhanced using the PRSA transform (4) while this peak is hidden in the classical spectrum of y (Fig.2(b)). Other examples illustrating the potential of the PRSA as a tool to improve the estimation of existing periodicities are provided in [8, 9]. In Appendix A, the relationship between a signal composed of a sum of sinusoids and its PRSA signal is derived.

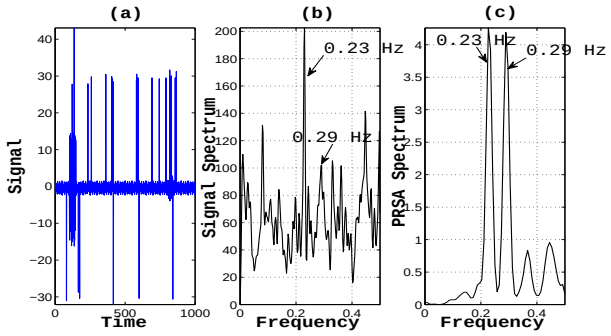

Figure 2: Enhancement of existing quasi-periodic components using the PRSA: (a) studied signal (5), (b) signal spectrum and (c) squared magnitude of the PRSA transform $|\tilde{Y}_q|^2$ (4).

2.2 Time-frequency representation based on the PRSA

In this section, we introduce a new time-frequency representation based on signal windowing and local application of PRSA. We aim both at exploring the ability of the PRSA to capture the local periodicities and at highlighting the time variation of the frequency components.

Let us consider a signal $\{x_k\}_{k=0,\ldots,K-1}$, where K is the sample size. A sequence $\{x_{k-K_w+1}, x_{k-K_w+2}, \ldots, x_k\}$ is obtained from this signal using a moving window of length K_w. For reasons of clarity, the considered sequence is locally denoted by y:

$$y_n = x_{k-K_w+n} \qquad \text{for} \qquad n = 1,2,\ldots,K_w. \tag{6}$$

The PRSA signal $\tilde{x}_{k,\ell}$ of this sequence and its PRSA transform $\tilde{X}_{k,q}$ are defined using (3) and (4) respectively by:

$$\tilde{x}_{k,\ell} = \tilde{y}_\ell \qquad \text{for} \qquad \ell = -L, -L+1, \ldots, L, \tag{7}$$

$$\tilde{X}_{k,q} = \tilde{Y}_q \qquad \text{for} \qquad q = 0,1,\ldots,Q-1. \tag{8}$$

By repeating the procedure for all $k = K_w, \ldots, K-1$, a time-frequency representation which describes the time-evolution of the frequency features of the signal is obtained (in analogy with the short-time Fourier transform and the spectrogram):

$$\begin{array}{ccccc} \text{Time} & \times & \text{Frequency} & \longrightarrow & \text{PRSA-TFR} \\ (k & , & q) & \longmapsto & \left|\tilde{X}_{k,q}\right|^2. \end{array} \tag{9}$$

In the following, examples illustrating the potential of the PRSA-TFR are presented and compared to classical TFRs, the SPWV distribution [1, 2], the spectrogram and the reassigned spectrogram [4].

3. PRSA-TFR VERSUS CLASSICAL TFRS - RESULTS AND DISCUSSIONS

3.1 Application to simulated signals

Let us consider simulated signals shown on Fig.3 (a), (b) and (c). The first signal is a sum of two sinusoid components (at constant frequencies 50 Hz and 160 Hz) and of a frequency-modulated component (linear modulation). These three components are embedded in an additive white Gaussian noise $AWGN$, the variance of which is $\sigma^2 = 16$, and an impulsive noise Imp of magnitude 40 and occurring with a probability

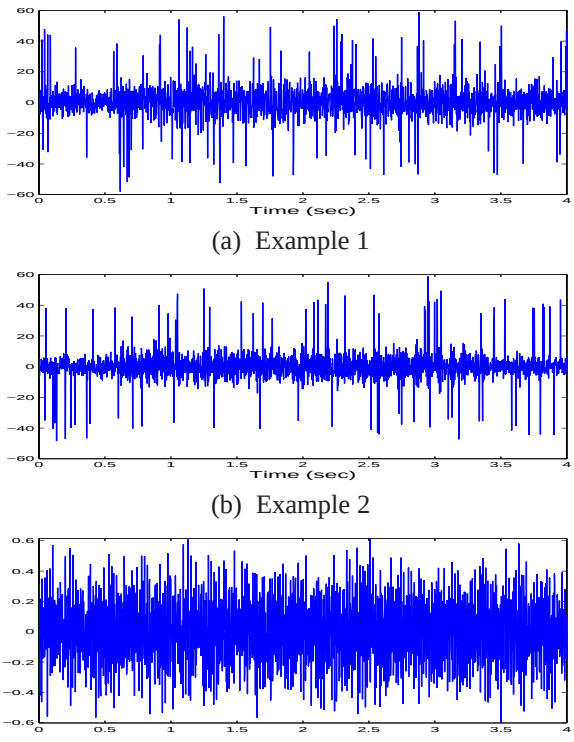

(a) Example 1

(b) Example 2

(b) Example 3

Figure 3: Examples of simulated signals. (a) signal composed of the sum of three components with linear frequency modulations and constant amplitudes. (b) signal composed of the sum of three components with nonlinear frequency modulations. (c) a nonlinear amplitude modulated signal.

of 21 spikes per sec:

$$\begin{aligned} y_1[n] &= 4\sin(2\pi 160n+\tfrac{\pi}{3})+ \\ &\quad 6\sin(2\pi 50n+\tfrac{\pi}{6})\mathbb{I}_{[0.8,3.4]}(n)+ \\ &\quad 6\sin\left(2\pi(0.02n^2+43.5n)+\tfrac{\pi}{8}\right)\mathbb{I}_{[0.6,3.9]}(n)+ \\ &\quad AWGN(n)+Imp(n). \end{aligned} \tag{10}$$

The second signal is the sum of three frequency-modulated components (nonlinear and exponentially decreasing modulation) of a constant amplitude equal to 4. These three components are, also, embedded in additive white Gaussian noise, the variance of which is $\sigma^2 = 12.25$ and an impulsive noise of magnitude 40 occurring with a probability of 21 spikes per sec.

The last example is that of a nonlinear amplitude modulated signal embedded in additive white Gaussian noise, the variance of which is $\sigma^2 = 0.04$:

$$y_3[n] = a(n)\,sin(2\pi\,136.5\,n)+AWGN(n), \tag{11}$$

where $a(n) = 0.21 + 0.2\,sin(2\pi\,51.5\,n)$. The sampling frequency in all cases is F_s =500 Hz.

In order to compare the classical TFRs with the PRSA-TFR, we consider the following details:

- For the PRSA-TFR, spectrogram and the reassigned spectrogram, the same size of the moving window is considered, $K_w = 300$.
- We ignore nonpositive values in the SPWV distribution in order to be able to have a representation in dB,

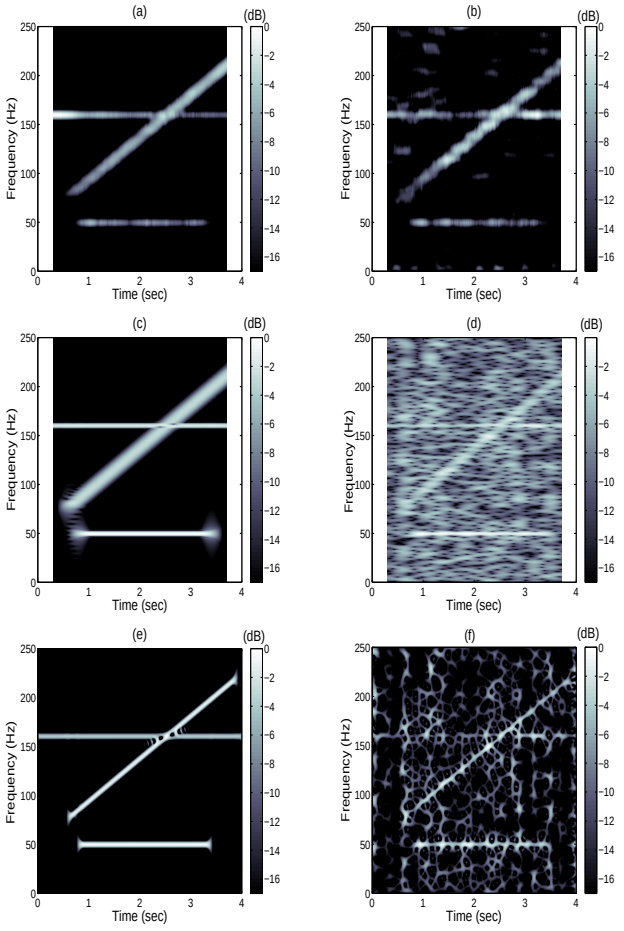

Figure 4: Example 1 of linear modulations: PRSA-TFR versus spectrogram and SPWV distribution. (a), (c) and (e) simulated signal without noise processed by PRSA-TFR, spectrogram and SPWV respectively. (b), (d) and (f) simulated signal corrupted by impulsive noise and AWGN noise processed by PRSA-TFR, spectrogram and SPWV respectively.

- all TFRs obtained are normalized by their maximum value and the same dynamic in dB is fixed to a threshold equal to -17 dB, for comparison purposes,
- the segments centered on the anchor points are $2L+1 = 131$ sample length and the DFT size is $Q = 1024$.

One can observe that the PRSA-TFR presents a slight decrease in time-frequency resolution, mainly induced by its construction. Indeed, the DFT is applied to the PRSA signal, the length of which is smaller than the moving window length. Despite this slight decrease in time-frequency resolution with the PRSA-TFR, one can distinguish the frequency components better than using classical TFRs with respect to a same fixed dynamic. The PRSA-TFR succeeds in removing the impulsive noise. In both examples with linear and nonlinear modulations, the frequency components are enhanced and the time-evolution of the frequencies clearly appears.

Now let us consider the signal of example 3. This signal can be rewritten as a sum of two signals embedded in additive white Gaussian noise. The first signal is a sinusoid at a constant frequency 136.5 Hz and having a constant ampli-

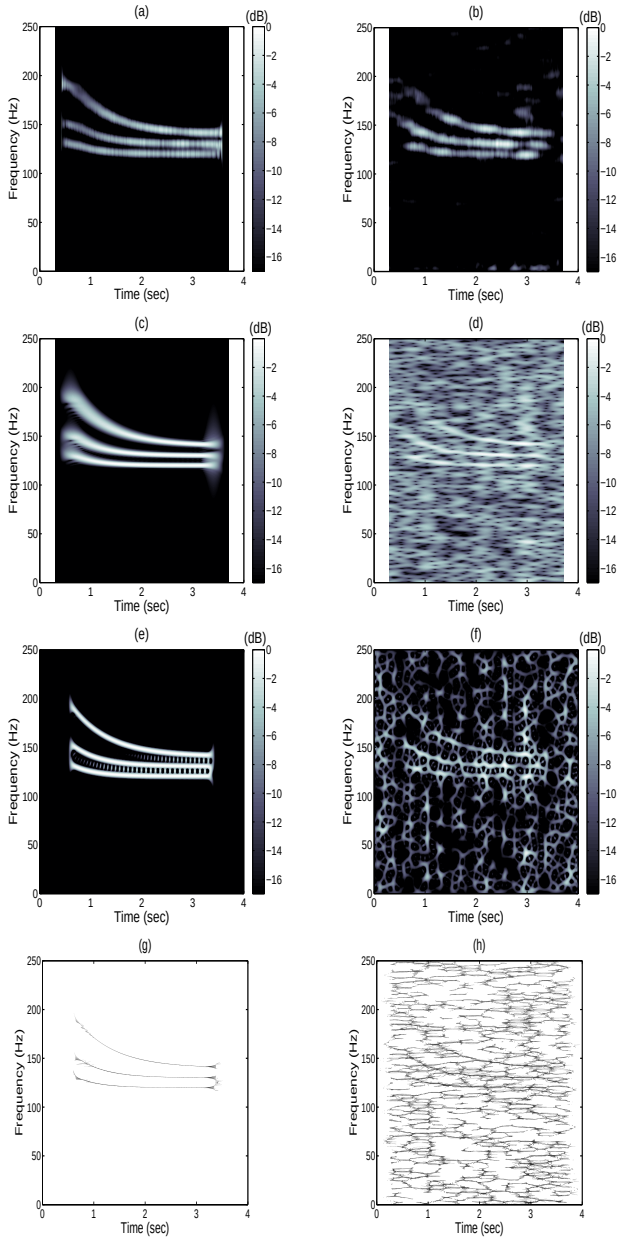

Figure 5: Example 2 of nonlinear modulations: PRSA-TFR versus spectrogram, SPWV distribution and reassigned spectrogram. (a), (c), (e) and (g) simulated signal without noise processed by PRSA-TFR, spectrogram, SPWV and reassigned spectrogram respectively. (b), (d), (f) and (h) simulated signal corrupted by impulsive noise and AWGN noise processed by PRSA-TFR, spectrogram, SPWV and reassigned spectrogram respectively.

tude equals to 0.21 while the second signal is the product of two sinusoids at frequencies 136.5 Hz and 51.5 Hz. This second signal contributes to the apparition of two components at frequencies 136.5 Hz$\pm$51.5 Hz in the spectrogram shown in Fig.6(b)). In contrast, one can see that in Fig.6(a), this second signal is canceled by the PRSA-TFR whereas the first signal is enhanced.

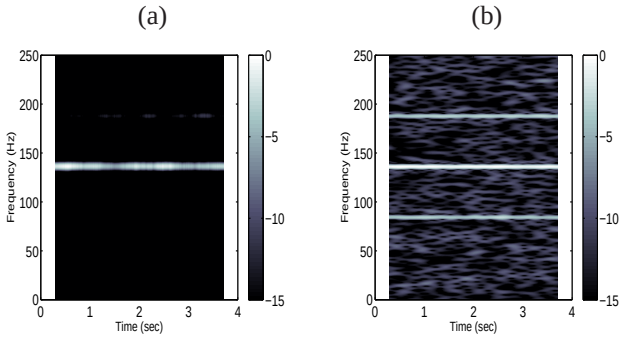

Figure 6: Example 3 of a nonlinear amplitude modulated signal: (a) PRSA-TFR versus (b) spectrogram.

3.2 Analysis of EEG signal using PRSA-TFR

The PRSA-TFR is compared to the spectrogram and the SPWV on an EEG signal. This signal was recorded on the right-sided parieto-occipital electrode PO4 during a visual recognition task. It is shown in Fig.7(a), where the vertical dashed line denotes stimulus onset. The sampling frequency is 500 Hz. The TFRs obtained with the PRSA, spectrogram and SPWV are shown in Fig.7(b), (c) and (d) respectively. The sliding window length is 400 and the PRSA length is 191. The time-frequency locations with significant energies are visible with each TFR. However the evolution of the oscillations is better described by the PRSA-TFR, and the various components are also easier to discriminate. For example the 90 Hz oscillation decreases in frequency after stimulus onset is clearly visible with the PRSA-TFR. Another event is the appearance of two oscillatory components with increasing frequencies between 40 and 60 Hz shortly after stimulus presentation, which is delineated by the PRSA-TFR. In contrast, with the spectrogram or the SPWV, it is more difficult to interpret this oscillation.

4. CONCLUSION AND PERSPECTIVES

We introduced a new time-frequency representation, called PRSA-TFR, by locally applying the PRSA on moving windows along the signal. This PRSA-TFR conserves the advantages of PRSA, which are mainly the attenuation of the noise level, especially with regard to impulsive noise, and the enhancement of quasi-periodic components. Despite a slight decrease in time-frequency resolution compared to classical TFRs, the PRSA-TFR makes the detection of dominant time-varying frequencies in nonstationary signals possible while noise level is decreased.

In future studies, we aim at studying the PRSA-TFR statistical features when applied to nonstationary signals, for segmentation and signal detection purposes.

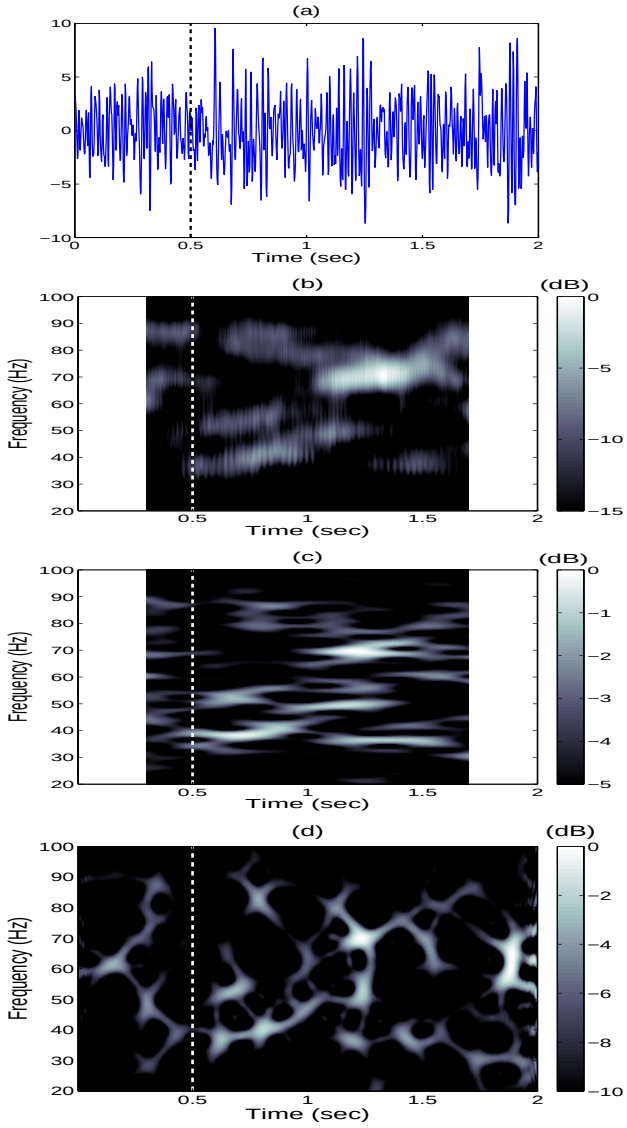

Figure 7: Example of EEG signal: PRSA-TFR versus spectrogram and SPWV distribution. (a) EEG signal, (b) PRSA-TFR, (c) spectrogram and (d) SPWV.

A. PRSA OF SINUSOIDAL MULTICOMPONENT SIGNAL

A short theoretical derivation of the average segment resulting from the application of PRSA to one single sinusoid signal is presented in [9]. This illustrates the contrast between the simplicity of the concept and the difficulty in extracting exact calculations. Here, we consider a signal composed of K sinusoidal components:

$$y_n = \sum_{k=1}^{K} a_k \sin(2\pi f_k\, n), \tag{12}$$

where a_k and f_k are the constant amplitude and frequency of the k^{th} component. According to (3), the PRSA signal of the signal of (12) is written :

$$\tilde{y}_\ell = \frac{1}{M} \sum_{m=1}^{M} \left(\sum_{k=1}^{K} a_k \sin\left(2\pi f_k\, (n_m + \ell)\right) \right). \tag{13}$$

which leads to the following expression :

$$\tilde{y}_\ell = \sum_{k=1}^{K} A_k \cos(2\pi f_k\, \ell) + B_k \sin(2\pi f_k\, \ell), \tag{14}$$

where

$$A_k = a_k \frac{1}{M} \sum_{m=1}^{M} \sin(2\pi f_k\, n_m) \tag{15}$$

$$B_k = a_k \frac{1}{M} \sum_{m=1}^{M} \cos(2\pi f_k\, n_m). \tag{16}$$

We remark that the PRSA signal (14) is still composed of K sinusoidal components, the frequencies of which are the same as those of the components of the original signal (12). However, their amplitudes A_k and B_k are proportional to the amplitudes a_k of the components of the original signal. For each component, the proportional factor ($\frac{A_k}{a_k}$ or $\frac{B_K}{a_k}$) is constant and only depends from the number of the anchor points M, the instant of anchor points n_m and the frequency f_k. This factor takes value in $[-1, 1]$, which explains the enhancement of some frequencies and the attenuation of some others.

REFERENCES

[1] L. Cohen, Time-frequency distributions - a review, Proceedings of the IEEE 77 (1989) 941–981.

[2] L. Cohen, Time-Frequency Analysis, Prentice-Hall, 1994.

[3] F. Auger, P. P. Flandrin, Generalization of the reassignement method to all bilinear time-frequency and time-scale representations, IEEE International Conference on Acoustics, Speech, and Signal Processing 4 (1994) 317–320.

[4] E. Chassande-Mottin, I. Daubechies, F. Auger, P. Flandrin, Differential reassignment, IEEE signal processing letters 4 (1997) 293–294.

[5] I. Djurovic, L. Stankovic, Robust wigner distribution with application to the instantaneous frequency estimation, IEEE Transactions on signal proc. 49 (2001) 2985–2993.

[6] F. Hlawatsch, A. Papandreou-Suppappola, G. F. Boudreaux-Bartels, The power classes quadratic time frequency representations with scale covariance and dispersive time-shift covariance, IEEE Transactions on signal processing 47 (1999) 3067–3083.

[7] A. Bauer, J. Kantelhardt, A. Bunde, P. Barthel, R. Schneider, M. Malik, G. Shmidt, Phase rectified signal averaging detects quasi-periodicities in non-stationary data, Physica A 364 (2006) 423–434.

[8] M. Lemay, Y. Prudat, V. Jacquemet, J. Vesin, Phase rectified signal averaging: A useful tool for the estimation of the dominant frequency in ECG signals during atrial fibrillation, in: Proceedings of the 29th Annual International Conference of the IEEE EMBS, Cite Internationale, Lyon, France, August 23-26, 2007.

[9] M. Lemay, Y. Prudat, V. Jacquemet, J. Vesin, Phase rectified signal averaging used to estimate the dominant frequencies in ECG signals during atrial fibrillation, IEEE on Transactions on biomedical eng. , TBME.2008.2001296.